Revealing the Aggregation Mechanism, Structure and Internal Dynamics of Poly(vinyl alcohol) Microgel Prepared through Liquid-Liquid Phase Separation

Marco Perfetti[a,b], Noemi Gallucci[a,b], Irene Russo Krauss[a,b], Aurel Radulescu[c], Stefano Pasini[c], Olaf Holderer[c], Gerardino D'Errico[a,b], Giuseppe Vitiello[d,b], Giulia Ottavia Bianchetti[e] and Luigi Paduano[a,b,*]

[a] Department of Chemical Sciences, Complesso Universitario Monte Sant'Angelo, University of Naples "Federico II", Via Cinthia, 80126, Naples, Italy.
[b] CSGI, Center for Colloid and Surface Science , 50019, Sesto Fiorentino, Italy.
[c] Forschungszentrum Jülich GmbH, Jülich Centre for Neutron Science JCNS, Outstation at Heinz Maier-Leibnitz Zentrum, Lichtenbergstraße 1, 85748, Garching, Germany.
[d] Department of Chemical, Materials and Production Engineering, University of Naples "Federico II", Piazzale Tecchio 80, 80125 Naples, Italy.
[e] Procter & Gamble Service Company NV/SA, Temselaan 100, 1853, Strombeek-Bever, Belgium.

Corresponding author: Luigi Paduano; luigi.paduano@unina.it

ABSTRACT: The use of technologies based on soft polymer particles represents an effective way to deliver target molecules with a specific function. In order to design a well performing delivery system, it is fundamental to rationalise both the aggregation and the structural properties of such particles.
In this study, we present the kinetic and structural characterization overtime of PVA nanogels obtained through a salting-out process in the presence of NaCl. We have analyzed how both polymer and salt concentration affect the aggregation process. The aggregation rate as well as the morphology and physico-chemical parameters such as mass and chain density of the nanogels have been determined through static and dynamic light scattering and discussed in the framework of the diffusion-limited and reaction-limited colloid aggregation. Insights into the polymer chains arrangements and their dynamics have been gained by means of small-angle neutron scattering and neutron spin echo measurements. As a result, it was found that the NaCl induce a liquid phase separation in solution with the formation of spherical PVA nanoaggregates, which grow under a reaction-limited aggregation mechanism. The particles increase their size and compactness over time. Within the aggregate, the polymer chains are locally organized to form randomly-oriented lamellae with a thickness of about 60 Å. The internal dynamics is a complex mixture of diffusion, Zimm dynamics and possibly effects from crowding with transition to a Rouse-like behavior.
The microparticle preparation based on the salting-out process constitutes a novelty, if compared to the methods already existing and based on the use of chemical crosslinkers, and is a cheap and easy protocol that allows tuning both particle size and density by varying the salt concentration.

1. INTRODUCTION

During the last years, an emerging interest has been devoted to the development of micro- and nano-structured materials for a wide range of applications in biomedicine, catalysis or environmental science. Specifically, soft polymer particles have been proposed as effective technologies to deliver target molecules with a precise function. Different protocols for the preparation of polymer-based delivery systems can be found in literature and the choice of a particular preparation method strictly depends on the final application.[1] Polyvinyl alchool, PVA, is among the most common species used for preparing polymer particles. This is thanks to its low-toxicity, non-carcinogenicity, good biocompatibility and desirable physical properties of the resulting particles such as rubbery or elastic nature and high degree of swelling in aqueous solutions.[2, 3] Furthermore, this copolymer is commercially available and can be obtained at low cost. It is possible to find many examples of vinyl alcohol-based particles in literature and several preparation protocols.[4] A model protein drug, bovine serum albumin (BSA), was successfully incorporated into injectable PVA hydrogel nanoparticles prepared by mixing of a BSA and a PVA solution to which silicon oil was further added.[2] Multiple freeing-thawing cycles on the mixture leaded to a suspension of PVA particles for biomedical applications. Acrylamine-functionalized PVA particles for wound healing application were prepared through UV cross-linking. The model drug used for this study was soybean trypsin inhibitor.[5] PVA particles can be also prepared through chemical cross-linking. Glutaraldehyde is the most common molecule used for this purpose. As an example, PVA microspheres were

prepared via inverse suspension-chemical cross-linking method.[6]

The main drawback of these existing method is the structural and/or chemical modification of the polymer used as a precursor, which does not allow keeping its original properties. At the same time, such methods are definitely more complex, if compared to the one here presented. Indeed, in this study we have focused on an easy and cheap particle preparation protocol, which differs from those reported in literature. Specifically, exploiting the ion-specific effect of the Hofmeister series on the macromolecule solubility, we have prepared PVA nanogels through a salting-out process by using NaCl. The preparation of PVA aggregates without the use of chemical cross-linkers does not modify the structure of the polymer, preserving its original properties of biocompatibility and biodegradability. The addition of a species that reduces the solubility of the polymer (known as cosmotropic species) triggers the polymer aggregation, inducing a local phase separation. As a result of such an aggregation, a colloidal dispersion is formed. In general, in colloid aggregation process two limiting regimes in the kinetics have been identified: a rapid, diffusion-limited colloid aggregation (DLCA) and a slow, reaction-limited colloid aggregation (RLCA).[7] A characteristic parameter to refer to discriminate between the two regimes is the fractal (Hausdorff) dimension, *d*. In three dimensions, the values of the fractal dimensions of structures formed by cluster aggregation were found to vary from d_{DLCA}= 1.7–1.8 to d_{RLCA} = 1.9–2.1.[8-10] The aggregation process in the two regimes leads to a different morphology of the aggregates, such as the degree of compactness, the shape and the amount of solvent within the particle. This in turn causes different physical and mechanical properties of the aggregates. The transition between DLCA and RLCA depends, among others, from parameters such as temperature,[11] pH,[12] particle and electrolyte concentration.[13]

Understanding the relationship between the aggregation regime and the corresponding morfological, microstructural and internal dynamic features is mandatory for any potential application of polymer nanogels in technological fields.

In this study we present a characterization of PVA nanogels formation in the presence of NaCl, discussing the kinetic growth within the framework of the DLCA and RLCA regime, and we show how both polymer and salt concentration affect the structural parameters of the aggregates obtained through salting-out. The kinetics of the clustering process is studied by mean of static and dynamic light scattering. During the process, the overtime evolution of several parameters such as mass, chain density and hydrodynamic radius of the aggregates is measured and discussed with respect to solute concentration and aggregation rate. The structural arrangement of the polymer chains within the aggregates is determinated through small-angle neutron scattering. Finally, on selected samples, neutron spin echo measurements allowed measuring the chain dynamics of the polymer inside the aggregates as the aggregation process occured.

2. EXPERIMENTAL SECTION

2.1. Materials

Poly(vinyl alcohol) (PVA) +99% hydrolyzed, mass average molecular weight 85000 ÷ 124000 g mol^{-1}, sodium chloride (NaCl, purity ≥ 99%, AR grade), sodium thiocyanate (NaSCN, purity ≥ 99.9%), potassium chloride (KCl, purity ≥ 99.0%) and calcium chloride ($CaCl_2$, purity ≥ 96.0%) were purchased from Sigma Aldrich (Milano, Italy) and used without further purifications. All aqueous solutions were prepared by using twice distilled Milli-Q water with the only exception of samples for neutron scattering and DLS, on pure PVA, measurements, where D_2O (Sigma) was used.

2.2. Samples preparation

A PVA stock solution was prepared by weighing the polymer and water into a glass vial. The vial was placed into a controlled temperature bath at 85 °C and the solution was kept under stirring at 700 rpm for 4 hours. The obtained solution was stored at room temperature (about 20 °C) for 1 hour. Stock salt solutions at different concentrations were prepared by adding the proper quantities of salt and water into the vial. In order to avoid the presence of dust particles, all solvents were filtered by using 0.20 μm filters. As shown below, concentrations of polymer and salt stock solutions were optimized for each set of samples to be prepared.[14]

For dynamic light scattering measurements, the samples were prepared by diluting a stock PVA 2% w/w solution with water and/or a stock salt 4.5 mol kg^{-1} solution. We kept the polymer concentration constant (1% w/w) and we studied 5 different NaCl concentrations (1.500 mol kg^{-1}, 1.625 mol kg^{-1}, 1.750 mol kg^{-1}, 1.875 mol kg^{-1} and 2.000 mol kg^{-1}).

For static light scattering measurements, 5 sets (of 5 samples each) at constant NaCl concentration and different polymer concentrations were prepared by diluting a stock aggregated PVA 1% w/w solution (i.e. a solution containing pre-formed aggregates) with NaCl stock solution at the same concentration. We studied 5 different NaCl concentrations: 1.500 mol kg^{-1}, 1.625 mol kg^{-1}, 1.750 mol kg^{-1}, 1.875 mol kg^{-1} and 2.000 mol kg^{-1}. At each NaCl concentration, 5 different PVA concentrations (0.20% w/w, 0.40% w/w, 0.60% w/w, 0.80% w/w and 1.00% w/w) were investigated.

Samples to be analyzed through transmission electron microscopy (TEM) were prepared by precipitations of the aggregates that were washed with distilled water at least ten times to eliminate the NaCl and then re-suspended in distilled water.

The samples prepared for small angle neutron scattering measurements were obtained by following the same procedure described above by using D_2O as solvent. We prepared a salt-free sample of PVA 1% w/w and 3 samples at constant PVA concentration (0.85% w/w) and at 3 different NaCl concentrations (1.500 mol kg^{-1}, 1.750 mol kg^{-1} and 2.000 mol kg^{-1}). For the neutron spin-echo (NSE) measurements, two samples were analyzed: PVA at 0.85% w/w in the presence of NaCl at 2.000 mol kg^{-1} at 4, 10 and 12 days from the preparation,

respectively, and PVA at 1.00% w/w in the presence of NaCl at 2.000 mol kg^{-1} at 4 days from the preparation.

2.3. Static Light Scattering (SLS) and Dynamic Light Scattering (DLS)

SLS and DLS measurements were performed by using a home-made instrument composed by a Photocor compact goniometer, a SMD 6000 Laser Quantum 50 mW light source operating at 532.5 nm, a photomultiplier (PMT-120-OP/B) and a correlator (Flex02-01D) from *Correlator.com* (see S.I.).[15, 16,17] All measurements were performed at 25 °C with the temperature controlled through a thermostatic bath.
In the case of SLS, we measured the scattering intensity at different scattering angles: 60°, 75°, 90°, 105° and 120°, whereas for the DLS measurements a fixed scattering angle of 90° was chosen.

2.4. Refractive index measurements

The refractive indexes of all solutions studied through SLS were measured by using an Abbe refractometer (Atago® NAR-3T, Bellevue, U.S.A.) operating at 25 °C by dropping 100 µL of solution between the illuminating and the refracting prisms. Each measurement was repeated three times and the average value of refractive index was calculated.

2.5. Small Angle Neutron Scattering (SANS)

SANS measurements were performed at 25 °C with the KWS-2 diffractometer operated by Julich Centre for Neutron Science at the FRMII source located at the Heinz Maier Leibnitz Centre, Garching (Germany). For all the samples, neutrons with a wavelength of 5 Å and $\Delta\lambda/\lambda \leq 0.1$ were used. A two-dimensional array detector at three different wavelength (W)/collimation (C)/sample-to-detector (D) distance combinations (W 5 Å/C 8 m/D 2 m, W 5 Å/C 8 m/D 8 m, and W 5 Å/C 20 m/ D 20 m) measured neutrons scattered from the samples. For sample containing only PVA the scattering intensity $I(q)$ was collected in the range of the modulus of the scattering vector $q = 4\pi n \sin(\theta/2)/\lambda$, between 0.08 $Å^{-1}$ and 0.4 $Å^{-1}$ and between 0.002 $Å^{-1}$ and 0.4 $Å^{-1}$ for the samples containing both PVA and NaCl. Here λ and θ represent the wavelength of the neutron beam and scattering angle, respectively (see S.I.).

2.6 Neutron spin-echo spectroscopy (NSE)

The reported experiments were performed using the J-NSE spectrometer "Phoenix" operated by Jülich Centre for Neutron Science (JCNS) at the research reactor FRM II of the Heinz Maier-Leibnitz Zentrum (MLZ) in Garching, Germany.[18] The samples were poured into quartz cells and measured at 25 °C. Measurements were performed at q-values of 0.03, 0.07, 0.1 and 0.15 Å, and at wavelength of 8, 10 and 13 Å.

2.7 TEM images

Samples of PVA nanogels were analyzed using transmission electron microscopy on a JEOL JEM-2100 (JEOL Ltd., Tokyo, Japan) operating at 200 kV. Approximately 50 µL of a given sample was applied to a carbon-coated copper grid and allowed to air dry.

3. RESULTS AND DISCUSSION

3.1. Aggregation properties of PVA

3.1.1. Aggregation and morphological properties of PVA in water. PVA can be dissolved in water up to 10% w/w, the maximum concentration here tested. Polymer aggregation was monitored by determining the diffusion coefficient of particles present in solution.[15] In the case of spherical objects, continuous medium and infinite dilution, the diffusion coefficient can be easily related to the hydrodynamic radius R_H through the Stokes-Einstein equation (details reported in S.I.):

$$R_H = \frac{k_B T}{6\pi\eta D} \qquad (3.1.1.1)$$

where k_B is the Boltzmann constant, T is the absolute temperature and η is the solvent viscosity. For non-spherical particles, R_H represents the radius of a spherical aggregate with the same measured diffusion coefficient. In this hypothesis, equation (3.1.1.1) can be reasonably used to estimate the averaged hydrodynamic radius of the particles.[19,20] The evolution of the hydrodynamic radius R_H over time obtained by DLS measurements for a 1% w/w PVA solution in D_2O is shown in Figure 1. We can notice the presence of a single population characterized by a hydrodynamic radius of 10.5 ± 0.5 nm.[21] Neither variation of R_H or additional populations were observed over time: this seems to indicate that no aggregation occurs over the 21 days of monitoring. It is to note that the measurements on pure PVA sample were performed in D_2O in order to compare the hydrodynamic radius obtained by DLS with the radius of gyration obtained by SANS.
The nature of the single population detected by DLS was revealed by performing SANS measurements on a PVA solution in heavy water at a polymer concentration of 1 % w/w. Figure 2 shows the neutron scattering intensity profile of PVA obtained after 2 days from the preparation. The Porod analysis in the high q-region, reported in the inset of Figure 2, shows a slope of -1.48 ± 0.01, close to the theoretical value of -5/3 = -1.667. This value is the signature of fully swollen coils,[22] thus we could assume that the PVA chains are highly hydrated. Two models are commonly used to describe solutions containing single polymer chains: the Debye model and the Polydispersed Gaussian Coil (PGC) model.[20] The former is used for gaussian polymer chains in theta solvent condition, which corresponds to the absence of either attractive or repulsive forces between the polymer coil and the solvent. The latter is used for gaussian polymer chains in good solvent condition, which corresponds to the high affinity of the polymer chain towards the solvent. Both models were tested on our data, and the best result was obtained by using the PGC model, represented by equation (3.1.1.2):

$$\frac{d\Sigma}{d\Omega} = I_0 \frac{2\left[\left(1+Ux\right)^{-1/U} + x - 1\right]}{\left(1+U\right)x^2} + bkg \qquad (3.1.1.2)$$

where $I_0 = \phi_{poly}\, V \left(\rho_{poly} - \rho_{solv}\right)^2$ with ϕ_{poly} is the polymer volume fraction, V is the volume of the scatterer, ρ_{poly} is the scattering length density of the polymer and ρ_{solv} is the scattering length density of the solvent; $x = R_g^2 q^2 / (1+2U)$ is the dimensionless chain dimension, depending on both the radius of gyration R_g and the polydispersity index $U = \left(M_w / M_n\right) - 1$. This model calculates an empirical functional form for the scattering from a polydisperse polymer chain assuming a Schulz-Zimm type molecular weight distribution.[20] The radius of gyration of the PVA chains in the investigated solution and the polydispersity were found to be 16.5 ± 0.2 nm and 3.6 ± 0.1 nm, respectively. It is well known that for single chain the R_H/Rg ratio should be about 0.665 for polymer in ideal/theta solvent. In the present case from our measurements the ratio is about = 0.64. Therefore, we can infer that the single population observed in DLS measurements corresponds to the free polymer chains.

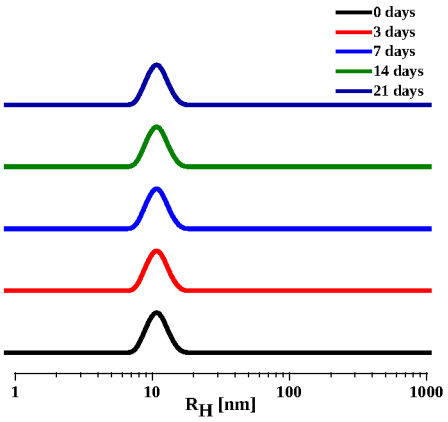

Figure 1. Distribution curves of hydrodynamic radii for PVA in D_2O at different times from the preparation of the polymer solution at a concentration of 1% w/w.

3.1.2. Aggregation process of PVA in the presence of NaCl. In order to study the effect of different salts on the aggregation properties of PVA, we performed a preliminary DLS study by using NaSCN, $CaCl_2$, KCl and NaCl, whose anions and cations belong to very distinct positions of the Hofmeister series. The obtained results are shown in the supporting information (see Figure S.2.2S): overall, NaCl was the only species that induced quantitative polymer aggregation over a timescale reasonable to perform a study. Therefore, we decided to draw our attention to the polymer aggregation process in the presence of NaCl, in order to study how the salt concentration affects both the aggregation kinetics and the structural properties of the PVA aggregates.

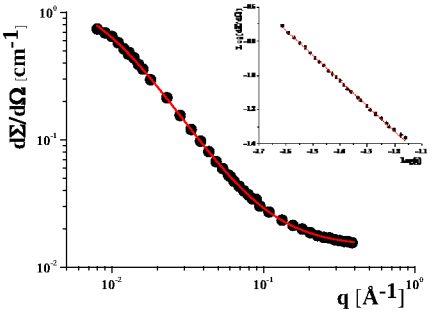

Figure 2. Neutron scattering intensity profile for PVA in D_2O after 2 days from the preparation at a concentration of 1% w/w; Porod analysis performed in the high *q*-region is reported in the inset. Experimental data are represented by black circles and fitting curves by red lines.

We carried out a time-dependent DLS analysis by varying NaCl concentration and keeping PVA concentration constant (1% w/w). We investigated the growth of the aggregates at 5 different NaCl concentrations: 1.500 mol kg^{-1}, 1.625 mol kg^{-1}, 1.750 mol kg^{-1}, 1.875 mol kg^{-1} and 2.000 mol kg^{-1}. DLS measurements were performed every day in order to monitor the evolution of the hydrodynamic radius over time. Results show that incubation of PVA in the presence of NaCl eventually results in polymer precipitation on a timescale which depends on salt concentration. In particular macroscopic polymer precitation was observed at shorter times for solution at higher salt concentrations: upon 46 days for 1.500 mol kg^{-1} NaCl, 26 days for 1.625 mol kg^{-1} NaCl, 15 days for 1.750 mol kg^{-1} NaCl, 9 days for 1.875 mol kg^{-1} NaCl, and 8 days for 2.000 mol kg^{-1} NaCl.

Figure 3 shows the evolution of the hydrodynamic radii over time for the samples at 1% w/w of polymer at 3 different NaCl concentrations (1.500 mol kg^{-1}, 1.750 mol kg^{-1} and 2.000 mol kg^{-1}); instead the other evolutions of hydrodynamic radii to other NaCl concentrations (1.625 mol kg^{-1} and 1.875 mol kg^{-1}) are shown in supporting information (see Figure S.2.3). All curves indicate the presence of both a first population at about 18 nm and a second one at a variable value ranging between 100 and 1000 nm, likely due to PVA aggregates, which appears at earlier times for higher NaCl concentrations. The complete conversion from free chains to aggregates is achieved upon 15-16 days for 1.500 mol kg^{-1} NaCl, 7-8 days for 1.625 mol kg^{-1} NaCl, 3-4 days for 1.750 mol kg^{-1} NaCl, 3 days for 1.875 mol kg^{-1} NaCl and 2-3 days for 2.000 mol kg^{-1} NaCl. Therefore, at all salt concentrations aggregation is observed and this process is faster at higher NaCl concentrations. Moreover, it is worth highlighting the presence of a further population that appears just before polymer precipitation, whose dimension ranges between 800 and 1200 nm. Only at NaCl 1.750 mol kg^{-1} this population is absent, but we can observe a single broad population. The presence of either this further population or a broad one is probably due to the coalescence of the aggregates, whose number becomes statistically relevant, leading to the formation

of a third population of "aggregates of aggregates". This phenomenon could explain the subsequent PVA precipitation, which is due to the increased aggregate size.

From the previous results we can observe that PVA shows an aggregation behavior in NaCl solutions

Similar to that already found for poly(ethylene vinyl alcohol), EVOH,[14] which differs chemically from PVA due to the presence of ethylene sequences along the polymer chain. However, whereas for EVOH precipitation occurs just after the formation of a single aggregate population, for PVA this process is slower and a monomodal distribution is present for about 4 days at 2.000 mol kg^{-1} and for about 25 days at 1.500 mol kg^{-1}. Precipitation can be clearly explained by hypothesizing coalescence among aggregates, as shown in Figure 4. In particular, free chain aggregation leads to the formation of bigger particles, whose dimensions grow over time by consecutive addition of free chains. At this step, both free chains and aggregates are present in solution and the scattering contributions are relevant for both populations. Then, when free chains are not statistically significant, their scattering contribution is definitely lower and only the aggregate population appears from DLS data. Nevertheless, at this stage, free chains are still present in solution and this explains why the growing process of the aggregates is still ongoing. Finally, when the aggregate number statistically increases, coalescence among bigger particles occurs, leading to polymer precipitatio

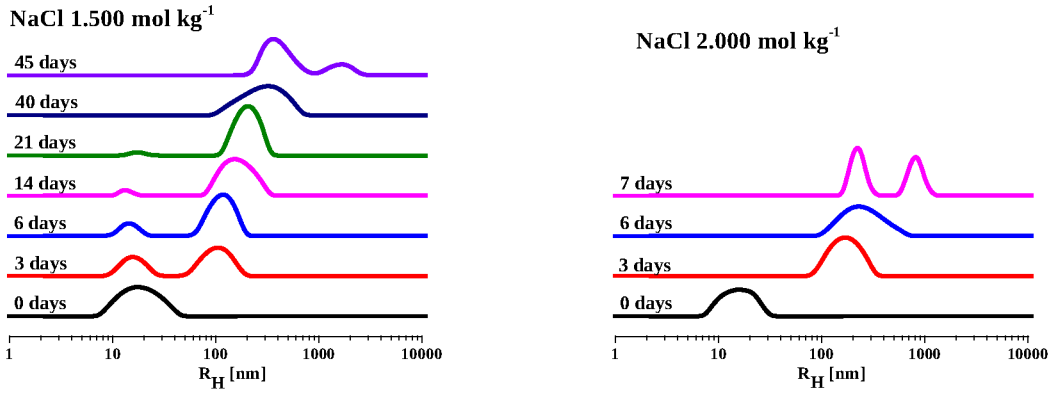

Figure 3. Evolution of hydrodynamic radii distributions over time by DLS for a PVA concentration of 1% w/w and for 2 different NaCl concentrations.

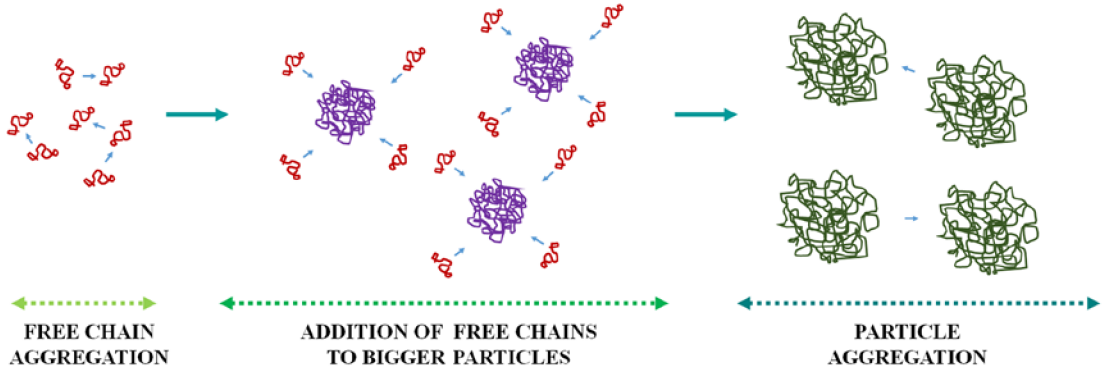

Figure 4. Sketch representation of the hypothetical PVA aggregation mechanism: violet particles are the result of the free chain aggregation, over time those also self-aggregate (green particles) forming large particles and eventually precipitate.

3.2. Structural properties of PVA aggregates.

3.2.1. TEM study. TEM measurements allowed us to gain structural information on PVA aggregates. Figure 5 shows a TEM image collected at 1.750 mol kg^{-1} NaCl and 1% w/w PVA after 3 days from preparation. By considering the previous results from DLS, such a time was chosen in order to obtain a picture of the system during the aggregation process, when both free chains and aggregates are present in solution. The image shows a polymer particle characterized by a "sponge-like" structure and by a radius of about 90 nm, which is in good agreement with the DLS data.

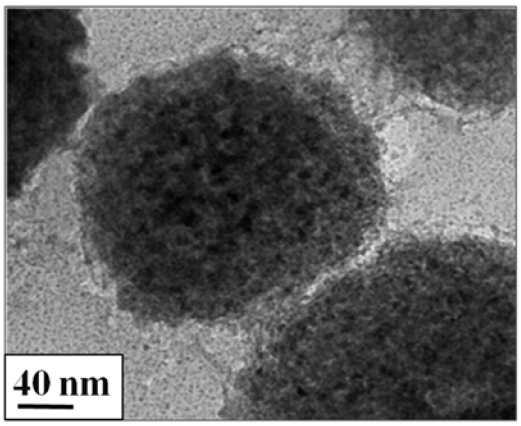

Figure 5. TEM image collected for 1% w/w PVA solution at 1.750 mol kg^{-1} NaCl concentration upon three days from preparation. The image highlights the "sponge-like" structure of the polymer nanogels.

3.2.2. Light Scattering study. In order to obtain further information on the structural properties of PVA aggregates, we estimated their average molar weight through SLS. Such measurements were performed for 1.500 mol kg^{-1}, 1.625 mol kg^{-1}, 1.750 mol kg^{-1} 1.875 mol kg^{-1} and 2.000 mol kg^{-1} NaCl, once a monomodal hydrodynamic radius distribution of polymer aggregates is obtained, as shown in Figure 3 and in Figure S.2.3 Dilution of the stock 1% w/w PVA aggregate solution, performed in order to have a set of samples at different polymer concentration for the SLS measurements, did not affect either the size or the particle radius distribution. This was confirmed by a preliminary gauging of the hydrodynamic radius of the aggregates (data not show). Since PVA aggregation occurs over a wide time scale, we were able to study the evolution of both the particle molar masses and structural parameters over time, by diluting the stock aggregate solution and repeating the SLS measurements every day until polymer precipitation. The relation between the scattering intensity, concentration of the scattering objects and scattering angle is:[23]

$$\frac{Kc}{R_\theta} = \frac{1}{M_w}\left[1 + \frac{q^2\left\langle R_g^2\right\rangle}{3} + 2A_2M_wc\right] \qquad (3.2.2.1)$$

where c is the concentration of the scattering objects and $K = \frac{1}{N_A}\left(\frac{2\pi n}{\lambda^2}\frac{dn}{dc}\right)^2$ is a constant that depends on the incident wavelength λ, the Avogadro number N_A, the solvent refractive index n and the variation of the solution refractive index with the polymer concentration dn/dc. When samples are highly diluted, it can be assumed that dn/dc does not change with the wavelength. The parameter q is the modulus of the scattering vector and θ represents the scattering angle. M_w, R_g and A_2 are the mass average molecular weight, the radius of gyration and the second virial coefficient for the scattering objects, respectively. Finally, R_θ is the Rayleigh ratio and represents the term of the equation where the scattering intensity appears. Its expression is:

$$R_\theta = \frac{\left(I_S - I_0\right)}{I_R}\frac{n_0^2}{n_R^2}R_{\theta,R} \qquad (3.2.2.2)$$

where I_S, I_o and I_R are the scattering intensities of the sample, the solvent and the reference (toluene), respectively, n_o is the refractive index of the solvent and n_R is the refractive index of the reference. $R_{\theta,R}$ is the Rayleigh ratio of the reference at the same incident wavelength, calculated by applying a formula reported in literature.[24] In the presence of big particles, typically with a radius > $\lambda/10$, the scattering intensity dependence on both concentration and scattering angle has to be taken into account. Therefore, the values of Kc/R_θ have to be plotted as a function of two independent variables, c and q, in order to obtain the so-called Zimm plot.[25] By extrapolating the values of Kc/R_θ at both null concentration and null angle (i.e. null scattering vector), it is possible to obtain two datasets that, once fitted, give the molecular weight, the second virial coefficient and the radius of gyration, as shown in the equations below:

$$\frac{Kc}{R_\theta} = \frac{1}{M_w} + 2A_2c \qquad \text{for } \theta = 0 \qquad (3.2.2.3)$$

$$\frac{Kc}{R_\theta} = \frac{1}{M_w}\left[1 + \frac{\left\langle R_g^2\right\rangle}{3}q^2\right] \qquad \text{for } c = 0 \qquad (3.2.2.4)$$

Each dataset was fitted at constant angle and constant concentration. As an example, the Zimm plots obtained for PVA particles at 3 different NaCl concentrations at a specific time from the preparation (27 days, 12 days and 4 days for 1.500 mol kg^{-1}, 1.750 mol kg^{-1} and 2.000 mol kg^{-1} NaCl, respectively) are shown in Figure 6; instead the Zimm plots obtained for PVA at 1.625 mol kg^{-1} and 1.875 mol kg^{-1} NaCl concentrations are shown in supporting information (see Figure S.2.4). The evolution of the aggregate molar weights and the hydrodynamic radii (from DLS measurements carried out on the same day of SLS measurements) over time are reported in supporting information (see Figure S.2.6 and Figure S.2.7, respectively). Moreover, from the values of R_H we

estimated the evolution of the chain density over time, expressed as number of polymer chains per unit of hydrodynamic volume. Results are shown in Figure 7. It is possible to observe a general increase of this parameter with aggregation time for all NaCl concentrations. Moreover, at higher NaCl concentrations, the chain density increases faster.

At the same time, if we compare the values of packing degree at different NaCl concentrations but at the same aggregation time (i.e. 5 days for 1.750 mol kg^{-1}, 1.875 mol kg^{-1} and 2.000 mol kg^{-1} NaCl) we can notice that this parameter is higher when salt concentration increases. This means that higher salt concentration leads to a more compact aggregate. Similar comparisons can be made for different datasets at distinct aggregation times.

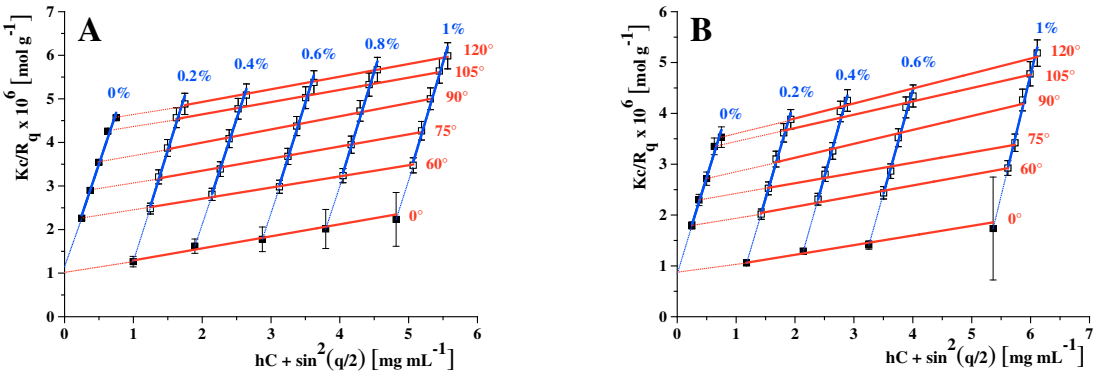

Figure 6. Zimm plots for PVA aggregates at 1.500 mol kg^{-1} and 2.000 mol kg^{-1} NaCl (panel A and B, respectively). Open squares indicate experimental data, straight blue lines and straight red lines represent the fitting curves at constant concentration and constant angle, respectively. Full squares indicate extrapolated points. Error bars were calculated as the standard deviation for 4 independent intensity measurements.

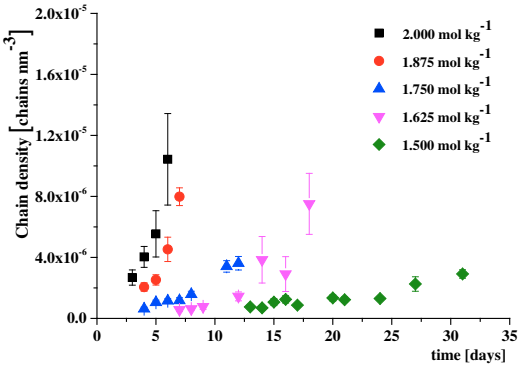

Figure 7. Evolution of aggregate chain density over time at 5 different NaCl concentrations. These results were obtained by combining SLS and DLS data.

3.2.3. Revealing the aggregation mechanism. From the data reported in Figure S.2.6, it is clear that at every NaCl concentration the aggregate molar weight shows an exponential increase with the aggregation time. In particular, the growth is faster at higher NaCl concentrations, as already shown by DLS data (reported in Figure S.2.7), for which we can observe a linear dependence of R_H on time. From the exponential dependence of M_w over time we can infer that the PVA aggregation occurs under a RLA (Reaction Limited Aggregation) mechanism[26]. In particular, the aggregation rate is given by the following expression:

$$k \approx v\, exp\left(V_b / k_B T\right) \qquad (3.2.3.1)$$

where V_b is the repulsive barrier between two approaching particles and v is the attempt frequency, which depends on the diffusive motion of the particles, as well as on their radius and concentration. When two particles approach each other closely on Brownian trajectories, the probability P of sticking increases with the aggregate mass. RLA typically occurs when $V_b \geq k_B T$, making k sufficiently small that there is a significant range of cluster size with $P << 1$, even though the attempt frequency, that depends on diffusion, remains high.[26] Once observed an exponential dependence of M_w on the aggregation time, experimental data reported in Figure S.2.6 were fitted by using a modified equation proposed by Ball *et al.*: [26]

$$M_w = A_0 + A exp\left(t / t_m\right) \qquad (3.2.3.2)$$

where A_o is the intercept at time = 0, A is the pre-exponential factor and t_m is a sample-dependent constant which is related to the aggregation rate. Interpolation of the experimental data was possible only for the datasets at 1.500 mol kg^{-1}, 1.625 mol kg^{-1} and 1.750 mol kg^{-1} NaCl, since a minimum number of experimental points was required for the fitting. The obtained t_m values are reported in table 1. We can observe a progressive decrease of this parameter with NaCl concentration, which indicates that the aggregation process is faster at higher NaCl concentrations.

3.2.4. Further structural information. The knowledge of the parameters derived from SLS measurements on PVA particle solutions allowed us to obtain further insights into the particle structure. In particular, the values of aggregate molar weight and gyration radius obtained from the Zimm plot analysis (whose examples are shown

in Figure 6 and in Figure S.2.4) at the same aggregation time were fitted for 3 different datasets (1.500 mol kg^{-1}, 1.625 mol kg^{-1} and 1.750 mol kg^{-1} NaCl) by applying the following equation, that allows the value of the shape parameter α to be obtained: [27]

$$R_g = BM_w^{\alpha} \qquad (3.2.4.1)$$

where B is a pre-exponential factor. This analysis was not carried out for 1.875 mol kg^{-1} and 2.000 mol kg^{-1} NaCl, due to the limited amount of available experimental points, which did not allow a reliable fitting to be performed. The value of parameter α gives information about the shape of the particle, for example the theoretical value for a spherical homogeneous particle is 0.33 [28], up to 1 in the case of a rod-like particle. The couples (M_w, R_g) derived from Zimm plot analysis at specific aggregation times are reported in Figure 8, where also interpolations are shown.

Values of α from the fittings reported in table 1 strongly indicate that PVA aggregates have a spherical shape characterized by a homogeneous density. This finding is coherent with the TEM image previously shown. Moreover, since α does not substantially change with NaCl concentration, we can deduce that salt concentration does not affect the shape of the particle.

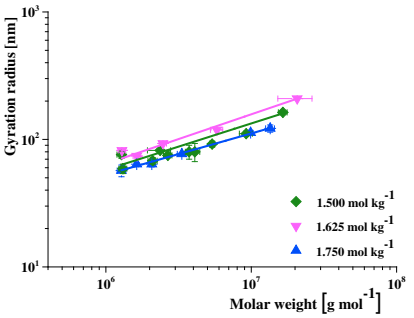

Figure 8. Dependence of gyration radius on aggregate molar weight at 3 different NaCl concentrations. The couples (M_w, R_g) derived from Zimm plot analysis at specific aggregation times were considered.

Table1. Values of t_m and α obtained from fittings of the data reported in Figure S.2.6 and Figure 10, respectively.

	NaCl 1.500 mol kg^{-1}	NaCl 1.625 mol kg^{-1}	NaCl 1.750 mol kg^{-1}
t_m [days]	7.4 ± 0.5	3.2 ± 0.2	2.8 ± 0.2
α	0.36 ± 0.02	0.39 ± 0.02	0.32 ± 0.02

3.2.5. SANS study. PVA samples in NaCl solutions were also analyzed by SANS, in order to obtain detailed structural information. The measurements were performed in D_2O for all samples: specifically, due to the isotopic effect we tested different polymer concentrations and as a result, we chose a lower PVA concentration (0.85% w/w) with respect to that used for DLS measurements, in order to have comparable aggregation times. Moreover, the use of D_2O as a solvent allowed obtaining a sufficiently high contrast even though polymer concentration was lower. SANS measurements were repeated at 3 different times from preparation, in order to shed light on possible morphological changes. At the same time, we were able to compare the evolution of the structural parameters with NaCl concentration, by choosing identical times from preparation for the samples at 1.500 mol kg^{-1} and 1.750 mol kg^{-1} NaCl (8 days) and for those ones at 1.750 mol kg^{-1} and 2.000 mol kg^{-1} NaCl (4 and 6 days).
The experimental profiles of the samples in NaCl were analyzed through a double approach that we have already presented elsewhere,[14] by separating the scattering data at low q-values and at intermediate and high q-values, respectively. The obtained scattering profiles of the samples in NaCl at low q-values were analyzed through the Kratky plot, in which $I(q)q^2$ is reported as a function of q.[29] In this type of plot, the q-value related to the maximum can be used to estimate the radius of gyration of the particles by applying the equation (3.2.5.1):

$$R_g = \frac{2\pi}{q} \qquad (3.2.5.1)$$

The experimental profiles of the samples in NaCl at intermediate and high-q values, due to the q^{-2} intensity decay, were fitted by using a lamellar form factor, shown in equation (3.2.5.2):

$$P(q) = \frac{2\Delta\rho^2}{q^2}\left(1 - \cos(q\delta)\right) \qquad (3.2.5.2)$$

where $\Delta\rho$ is the neutron contrast and δ is the lamellar thickness. This model relates to the scattering intensity for a lyotropic lamellar phase where a uniform scattering length density and random distribution in solution are assumed.[30,31] Thickness polydispersity was also considered in the fitting by assuming a Schulz distribution.
Figure 9 shows the data and the related fittings of the sample at 2.000 mol kg^{-1} NaCl concentration, instead the SANS curves for the other NaCl concentrations (1.500 mol kg^{-1} and 1.750 mol kg^{-1}) are shown in supporting information (see Figure S.2.8). By applying the lamellar model, we assumed that the PVA particles are formed according to the same mechanism we already proposed

for EVOH, which assumes that aggregates are spherical particle composed by small randomly oriented lamellae formed during the aggregation process and interacting via hydrogen bonding.[14] Since PVA aggregation occurs over a wide time scale, we were able to study the effect of both aging and salt concentration on the lamellar thickness. Results of fitting are reported in table 2 and show that the thickness increases with time for the samples at 1.500 mol kg^{-1} NaCl, whereas for the samples at higher concentration such a trend is not observed. Thus, we could infer that for 1.750 mol kg^{-1} and 2.000 mol kg^{-1} NaCl, a maximum threshold value of thickness is reached after 4 days and 2 days from preparation, respectively. At higher salt concentrations the aggregation process seems to be fast enough to avoid a further thickening of the preformed lamellae and to allow the approach of free polymer chains and the consequent growth of a new lamella oriented differently from the ones previously formed that already compose the particle. As regards the effect of NaCl concentration for same age samples, we observe an increase of the thickness by comparing the samples at 1.500 mol kg^{-1} and at 1.750 mol kg^{-1} NaCl. An example of the Kratky plot analysis for the dataset at 1.500 mol kg^{-1} NaCl is reported in Figure 10, and the results are shown in table 2. For some samples this analysis was not possible because the maxima of the curves were out of the investigated q-range. In general, we can observe a progressive increase of the radii of gyration with NaCl concentration and time.

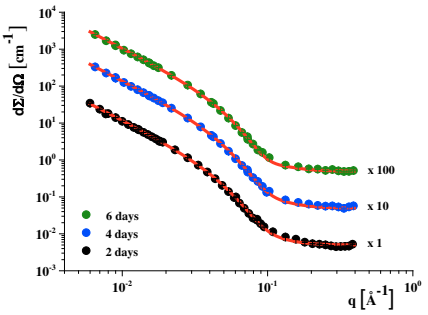

Figure 9. SANS data and fittings at 0.85% w/w PVA and 2.000 mol kg^{-1} NaCl and 3 different times from preparation.

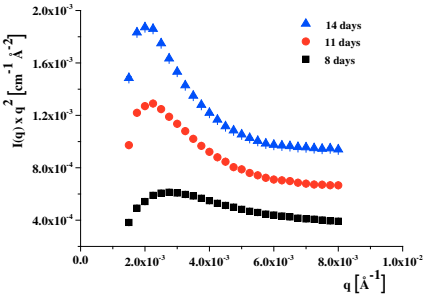

Figure 10. Kratky plots at 1.500 mol kg^{-1} NaCl and 3 different times from preparation.

Table 2. Structural parameters obtained from SANS fittings and Kratky plot analysis. Errors on lamellae thickness and related polydispersity are derived from the fitting, whereas the error on R_g was estimated by considering the standard deviation on this parameter calculated by considering a point adjacent to the maxima of the curves whose examples are shown in Figure 10.

1.500 mol kg^{-1} NaCl	**8 days**	**11 days**	**14 days**
Thickness [Å]	49.4 ± 0.2	57.5 ± 0.3	61.4 ± 0.1
polydispersity	0.61 ± 0.03	0.57 ± 0.03	0.32 ± 0.02
R_g [nm]	228 ± 18	280 ± 30	310 ± 30
1.750 mol kg^{-1} NaCl	**4 days**	**6 days**	**8 days**
Thickness [Å]	59.9 ± 0.1	60.1 ± 0.2	61.6 ± 0.2
polydispersity	0.28 ± 0.02	0.44 ± 0.01	0.24 ± 0.03
R_g [nm]	280 ± 40	470 ± 40	-
2.000 mol kg^{-1} NaCl	**2 days**	**4 days**	**6 days**
Thickness [Å]	59.7 ± 0.3	58.7 ± 0.2	58.4 ± 0.3
polydispersity	0.31 ± 0.01	0.29 ± 0.02	0.25 ± 0.03

3.2.6 Dynamics of chain within aggregate structure. A few preliminary measurements were performed on selected PVA nanogels by means of the spin-echo technique (NSE). The aim was to gain information on the diffusion

of polymer chains in the aggregates upon gelation process.

Measurements have been performed for the system at 0.85% w/w of polymer in the presence of NaCl at 2.000 mol kg^{-1} for 8, 10 and 13 Å, in a q-range between 0.03 $Å^{-1}$ and 0.2 $Å^{-1}$ (0.15 $Å^{-1}$), at temperature of 25°C. These concentrations were chosen in order to have quite slow aggregation rates suitable for typical measuring times of the neutron spin-echo experiment. The samples were mounted in a temperature-controlled sample environment. To our knowledge it is the first time this kind of systems are studied by means of the neutron spin-echo technique. The sample has been measured at three different times: 4, 10 and 12 days from preparation. The cell containing the polymer has never been opened during the whole experiment. During the measurement the average amplitude of the echo remained constant, a sign that the polymer was stable enough for NSE. The background, NaCl at 2.000 mol kg^{-1} in D_2O, has been subtracted from the experimental data, the latter have been then reduced with *DrSpine*, a new software for data reduction for spin-echo results.[32] The intermediate scattering functions of the PVA at 0.85% w/w are shown in Figures 11 as a function of the Fourier-time (τ), which is tuned to match the time-scale of the dynamics of the sample. The curves at 4 days are compared with those at 10 and 12 days: they decay faster than the others, a sign that the dynamics of the polymer chains slow down as the aggregation goes on. More pronounced differences are seen for larger values of q while for q=0.03 $Å^{-1}$ only the data for 12 days show an appreciable modification of the dynamics. Ideally, immediately after the polymer solution is prepared and the chains have not yet started to aggregate one would expect, as main contribution, a center-of-mass diffusion at smaller q's and a Zimm-like dynamics at larger wave vectors, due to hydrodynamic interactions. Typically a stretched exponential of the form:

$$\frac{S(q,\tau)}{S(q,0)} = A\exp\left\{-\left[\tau/\tau_0(q)\right]^{\beta}\right\} \qquad (3.2.6.1)$$

can describe this scenario quite well. Here the intensity A is fixed to 1 and $\tau_0(q)$ is fitted. For NSE the exponent β is typically 0.85 for Zimm dynamics.[33] Then the diffusion constant is given by:

$$D_{eff}(q) = \frac{\beta}{\tau_0(q)\Gamma(1/\beta)q^2} \qquad (3.2.6.2)$$

where $\Gamma(1/\beta)$ is the Gamma function. If plotted against q, $\tau_0(q)$ will be constant for the center-of-mass-diffusion and it will scale linearly with q for Zimm dynamics. The diffusion coefficients obtained for β =0.85 are shown in Figure 12. We observe that only the sample at 4 days presents a center-of-mass-diffusion at small q, which seems to be lost for the samples at 10 and 12 days, or presumably it is shifted to much smaller scattering vectors. At larger q's the PVA at 4 days presents a linear dependence with q. This is not the case for PVA at 10 and 12 days for which it seems that $\tau_0(q)$ has a non-linear power-law behavior. Thus, the scenario for these two samples is more complicated due to the presence of different dynamical regimes. In general, we observe that a single exponential function is not enough to describe all the NSE curves, as shown from the fits in Figure 11. It is reasonable to think that, as times passes by, aggregates of different sizes and single chains might coexist in the solution. In Figure 13 the logarithms $ln[S(q,\tau)/S(q,0)]$ is plotted for the 10-days sample. The log-log scale in the plot emphasizes the power-law behavior of the NSE curves: for PVA at 10 and 12 days we do not observe any simple Zimm-behavior, but a complex mixture of diffusion, Zimm dynamics with the β =0.85 slope and possibly effects from crowding with transition to a Rouse-like behavior similar to a "melt" with a β =0.5 dependence. More measurements are needed to both confirm these observations and to allow for the formulation of a model that can describe the data. In particular, in terms of the internal dynamics, it would be useful to have a comparison with the bulk PVA, i.e. a stable polymer solution with no aggregation process.

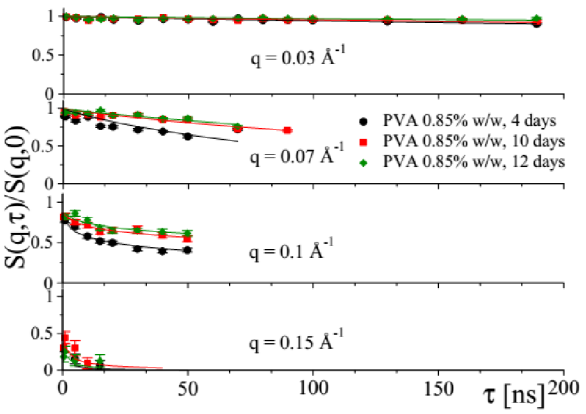

Figure 11. NSE intermediate scattering functions for PVA at 0.85% w/w at (•) 4 days, (■) 10 days, (♦) 12 days. The curve have been fitted with a stretched exponential as explained in the text.

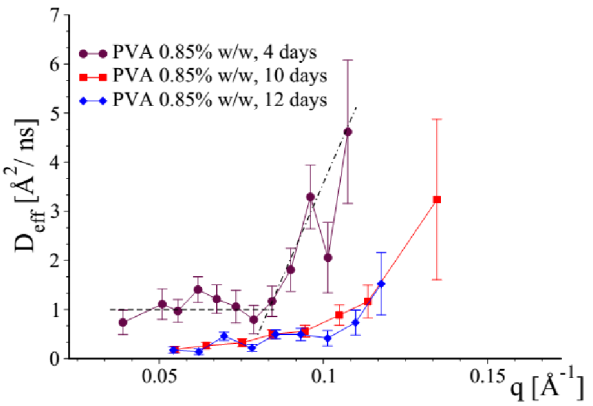

Figure 12. Diffusion coefficients for PVA at 0.85% w/w at different days obtained from eq. (3.2.6.2) with β=0.85. The point where the dashed (COM-dynamics) and the dashed-dotted (ZIMM-dynamics) lines meet sets the length scale where the internal dynamics starts to matter.

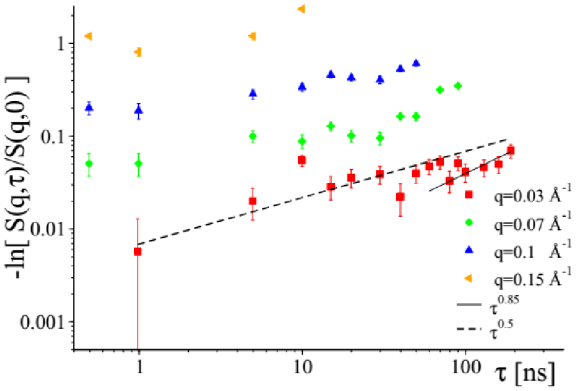

Figure 13. Slopes of the NSE data for PVA 0.85% w/w at 10 days. The lines provide a comparison with some power-laws that best fit the experimental data.

4. CONCLUSIONS

In this work we have presented the rationalization of the aggregation process of PVA in the presence of NaCl as a salting-out agent. The effect of both polymer and salt concentration on the kinetic and structural parameters of the aggregates have been studied. NaCl concentration directly affects the PVA aggregation rate and the nanogel morphology, whereas polymer concentration mainly affects the aggregate size. The PVA aggregation upon increasing salt concentration occurs under a RLA (Reaction Limited Aggregation) mechanism, which leads to an increasing polymer density that reflects in a more compact aggregate. The radius of gyration of the aggregates over time follows a power-law with their molecular weight with an exponent quite close to 0.33, typical of spherical homogeneous particles, a result confirmed by TEM images.

During the growth of the nanogel the single PVA chains probably go through a conformational change in order to maximize the H-bound interactions and to form randomly oriented lamellae with a thickness of about 60 Å. The internal dynamics, although not yet understood, suggests different dynamical regimes over time. At the initial times of the aggregation process the dynamics of the polydispersed system is characterized by the diffusion of the center of mass of the aggregated chains and by a Zimm-like dynamics at shorter length scales. However, as time goes by, more and more monomers and dimers are "eaten up" by larger agglomerates and the landscape of the motions evolves towards a more complex and more heterogeneous dynamical scenario. The diffusion of the larger particles is shifted towards smaller q's and this leaves room for the observation of the internal dynamics of the agglomerate. These first results suggest a mixture of very slow diffusion, of Zimm-dynamics and possibly of fast (segmental) motions of the aggregates chains resembling that of a "melt".

PVA particles prepared through salting-out are formed following an easy protocol, which does not require the use of chemical cross-linkers and that guarantees, at the same time, a compact structure where hydrogen bonding represents the main interaction among polymer chains. Moreover, the obtained polymer microdomains can be easily tuned from a structural viewpoint, by changing both PVA and NaCl concentration and can be used to host guest molecules. Therefore, the present study provides a useful piece of information that is fundamental in order to design a carrier system able to segregate target molecules (i.e. drugs, pollutants) for applications in biomedicine, environmental remediation or catalysis.

Acknowledgments

This work is based upon experiments performed at the KWS2 and J-NSE instruments operated by JCNS at the Heinz Maier-Leibnitz Zentrum (MLZ), Garching, Germany. Some of the authors LP, MP, and GV gratefully acknowledge the financial support provided by JCNS to perform the neutron scattering measurements at the Heinz Maier-Leibnitz Zentrum (MLZ), Garching, Germany.

REFERENCES

1. Ruocco, N.; Frielinghaus, H.; Vitiello, G.; D'Errico, G.; Leal, L. G.; Richter, D.; Ortona, O.; Paduano, L. *J Colloid Interf Sci* **2015,** 452, 160-168.
2. Li, J. K.; Wang, N.; Wu, X. S. *J Control Release* **1998,** 56, (1-3), 117-126.
3. Wang, A. H.; Xu, C.; Zhang, C. W.; Gan, Y. N.; Wang, B. *J Nanomater* **2015,** 1-8.
4. Paradossi, G.; Cavalieri, F.; Chiessi, E.; Spagnoli, C.; Cowman, M. K. *J Mater Sci-Mater M* **2003,** 14, (8), 687-691.
5. Bourke, S. L.; Al-Khalili, M.; Briggs, T.; Michniak, B. B.; Kohn, J.; Poole-Warren, L. A. *Aaps Pharmsci* **2003,** 5, (4).
6. Fei l.: Lili Y., L. Y. J. Z. *Journal of Applied Sciences* **2013,** 13, (14).
7. Lin, M. Y.; Lindsay, H. M.; Weitz, D. A.; Ball, R. C.; Klein, R.; Meakin, P. *Phys Rev A* **1990,** 41, (4), 2005-2020.
8. Lin, M. Y.; Lindsay, H. M.; Weitz, D. A.; Ball, R. C.; Klein, R.; Meakin, P. *Nature* **1989,** 339, (6223), 360-362.
9. Lin, M. Y.; Lindsay, H. M.; Weitz, D. A.; Ball, R. C.; Klein, R.; Meakin, P. *P Roy Soc Lond a Mat* **1989,** 423, (1864), 71-87.
10. Lindsay, H. M.; Klein, R.; Weitz, D. A.; Lin, M. Y.; Meakin, P. *Phys Rev A* **1989,** 39, (6), 3112-3119.
11. Tang, P.; Colflesh, D. E.; Chu, B. *J Colloid Interf Sci* **1988,** 126, (1), 304-313.
12. Carpineti, M.; Ferri, F.; Giglio, M.; Paganini, E.; Perini, U. *Phys Rev A* **1990,** 42, (12), 7347-7354.
13. Burns, J. L.; Yan, Y. D.; Jameson, G. J.; Biggs, S. *Langmuir* **1997,** 13, (24), 6413-6420.
14. Perfetti, M.; Krauss, I. R.; Radulescu, A.; Ruocco, N.; D'Errico, G.; Bianchetti, G. O.; Paduano, L. *Polymer* **2018,** 137, 122-131.
15. Simeone, L.; Mangiapia, G.; Irace, C.; Di Pascale, A.; Colonna, A.; Ortona, O.; De Napoli, L.; Montesarchio, D.; Paduano, L. *Mol Biosyst* **2011,** 7, (11), 3075-3086.
16. Della Vecchia, N. F., Luchini, A., Napolitano, A., D'Errico, G., Vitiello, G., Szekely, N., d'Ischia, M., Paduano, L. *Langmuir : the ACS journal of surfaces and colloids* **2014,** 30, 9811-9818.

17. Luchini, A., Irace, C., Santamaria, R., Montesarchio, D., Heenan, R. K., Szekely, N., Flori, A., Menichetti, L., Paduano, L. *Nanoscale* **2016,** 8, 10078-10086
18. Pasini, S.; Holderer, O.; Kozielewski, T.; Richter, D.; Monkenbusch, M. *Rev Sci Instrum* **2019,** 90, (4), 1-8.
19. Berne, B. J., Pecora, R., *Dynamic Light Scattering: With Applications to Chemistry, Biology*. Couvire Dover Publications: 2003.
20. Higgins, J. S., Benoit, H. C., *Polymers and Neutron Scattering*. Clarendon Press: 1997.
21. Ricciardi, R.; Mangiapia, G.; Lo Celso, F.; Paduano, L.; Triolo, R.; Auriemma, F.; De Rosa, C.; Laupretre, F. *Chem Mater* **2005,** 17, (5), 1183-1189.
22. Hammouda, B., Worcester, D. *Biophys J.* **2006,** 91, 2237–2242.
23. Johnson, C. S., Gabriel, D. A., *Laser Light Scattering*. Dover Publications: 1995.
24. Wu, H. *Chemical Physics* **2010,** 367, 44-47.
25. Zimm, B. H. *J. Chem. Phys.* **1948,** 16, 1093-1098.
26. Ball, R. C., Weitz, D. A., Witten, T. A., Leyvraz, F. *Physical review letters* **1987,** 58, 274-277.
27. Fourmaux-Demange, V., Boué, F., Brûlet, A., Keller, P., Cotton, J. P. *Macromolecules* **1998,** 31, 801-806.
28. Villegas, J. A., Cervantes, J. *J Inorg Organomet Polym* **2011,** 21, 157-164.
29. Burchard, W. *Macromolecules* **1977,** 10, 919-927.
30. Nallet, F., Laversanne, R., Roux, D. *J. Phys. II France* **1993,** 3, 487-502.
31. Berghausen, J., Zipfel, J., Lindner, P., Richtering, W. *J. Phys. Chem. B* **2001,** 105, 11081-11088.
32. Zolnierczuk, P. A., Holderer O., Pasini S., Kozielewski T., Stingaciu, L.R., and Monkenbusch M. *J. Appl. Cryst.* **2019,** 52, 1022-1034.
33. Richter, D.; Monkenbusch, M.; Arbe, A.; Colmenero, J. *Adv Polym Sci* **2005,** 174, 1-221.